

# Evidence for Dust Related X-ray Emission from Comet C/1995 O1 (Hale–Bopp)<sup>1</sup>

Alan Owens, A. N. Parmar, T. Oosterbroek, A. Orr  
Astrophysics Division, Space Science Department of ESA, ESTEC, 2200 AG Noordwijk,  
The Netherlands

L. A. Antonelli, F. Fiore<sup>2</sup>  
*BeppoSAX* Science Data Center, Nuova Telespazio, via Corcolle 19, I-00131 Roma, Italy

R. Schulz  
Solar System Division, Space Science Department of ESA, ESTEC, 2200 AG Noordwijk,  
The Netherlands

G. P. Tozzi  
Osservatorio Astrofisico di Arcetri, Largo E. Fermi 5, I-50125, Firenze, Italy

M. C. Maccarone  
IFCAI/CNR, via U. La Malfa 153, I-90146, Palermo, Italy

and

L. Piro  
IAS/CNR, via Enrico Fermi 21-23, I-00044, Frascati, Italy

## ABSTRACT

We report the discovery of X-ray emission from comet C/1995 O1 (Hale-Bopp) by the LECS instrument on-board *BeppoSAX* on 1996 September 10–11. The 0.1–2.0 keV luminosity decayed by a factor of 2 on a timescale of  $\sim 10$  hr with a mean value of  $5 \times 10^{16}$  erg s<sup>-1</sup>. The spectrum is well fit by a thermal bremsstrahlung model with a temperature of  $0.29 \pm 0.06$  keV, or a power-law with a photon index of  $3.1 \pm_{0.2}^{0.6}$ . The lack of detected C and O line emission places severe constraints on many models for cometary X-ray emission, especially those which involve X-ray production in cometary gas. The luminosity is a factor of at least 3.4 greater than measured by *Extreme Ultraviolet Explorer*

---

<sup>1</sup>Partially based on observations carried out at the European Southern Observatory (ESO), La Silla, Chile

<sup>2</sup>and Osservatorio Astronomico di Roma, I-00044, Monteporzio, Catone, Italy

(*EUVE*) 4 days later. This difference may be related to the emergence from the nucleus on 1996 September 9 of a dust-rich cloud. Over the next few days the cloud continued to expand becoming increasingly tenuous, until it had reached an extent of  $\sim 3 \times 10^5$  km (or  $\sim 2'$ ) by the start of *EUVE* observation. We speculate that the observed reduction in X-ray intensity is evidence for dust fragmentation. These results support the view that cometary X-ray emission arises from the interaction between solar X-rays and cometary dust.

*Subject headings:* comets: general — comets: individual (Hale-Bopp) — X-rays: general

## 1. INTRODUCTION

The *ROSAT* observations of X-ray emission from comets C/1996 B2 (Hyakutake) and C/1990 N1 (Tsuchiya-Kiuchi) came as a considerable surprise (Lisse et al. 1996; Dennerl et al. 1996b) and despite considerable effort there is still no generally accepted model for cometary X-ray emission. The emissions were centered a few arc-minutes ( $\sim 2 \times 10^4$  km) from the nucleus and had an extent of 5–15', or  $(3-8) \times 10^4$  km, being elongated normal to the Sun-nucleus line. The observed fluxes are a factor of  $\sim 10^3$  greater than predicted by early models in which X-rays are generated by fluorescent emission and scattering of solar X-rays in the coma (see Krasnopolsky (1997) for a review). Models which generate X-rays in the coma via solar wind proton, or electron, interactions also suffer from low efficiencies. In view of these difficulties, several models have emerged which predict higher cometary X-ray intensities (see Table 1). In the solar wind models of Häberli et al. (1997) and Cravens (1997) X-rays are generated following charge exchange excitations of highly ionized solar wind ions with neutral molecules in the comet's atmosphere. Bingham et al. (1997) propose that cometary X-rays are produced by energetic electrons generated by plasma wave turbulence. The turbulence is assumed to result from the relative motion of the cometary plasma and the solar wind. The attogram dust models of Wickramasinghe & Hoyle (1996) and Krasnopolsky (1997) produce X-rays from the scattering, fluorescence and bremsstrahlung of solar X-rays in attogram ( $\sim 10^{-18}$  g) dust particles, such as those detected in the wake of comet Halley (Utterback & Kissel 1990). Recently sub-micron sized grains have been observed in the coma of Hale-Bopp (Williams et al. 1997).

At the time of the *BeppoSAX* observation, Hale-Bopp (C/1995 01; Hale & Bopp 1995) was 2.87 AU from the Earth at a heliocentric distance of 3.13 AU and at a relatively constant brightness of  $m_v \sim 6$ . The Sun was at a Position Angle of  $274^\circ$  and the comet

phase angle (Sun-comet-Earth angle) was  $18^{\circ}7'$ . The size of the coma was estimated to be  $\sim 20'$  ( $\sim 2.5 \times 10^6$  km) and some observers reported a short dust tail of up to  $1^{\circ}5'$  ( $10^7$  km). The diameter of the nucleus is estimated by the *Hubble Space Telescope* to be 27–42 km (Weaver et al. 1997). In 1996 September Hale-Bopp was observed by the *Extreme Ultraviolet Explorer* (*EUVE*), *ROSAT*, *ASCA*, and *BeppoSAX* satellites. We present here results from the *BeppoSAX* observation briefly reported in Owens et al. (1997). Results from *ASCA* can be found in Kellett et al. (1997) and *EUVE* in Mumma et al. (1997) and Krasnopolsky et al. (1997a).

## 2. X-RAY OBSERVATION

The Low Energy Concentrator Spectrometer (LECS, 0.1–10 keV, Parmar et al. 1997) is one of five instruments on-board *BeppoSAX* (Boella et al. 1997a). It comprises an imaging mirror system and a driftless gas scintillation proportional counter. The energy resolution is 32% at 0.28 keV, the field of view (FOV) is  $37'$  diameter ( $4.6 \times 10^6$  km at the comet) and the full width at half-maximum (FWHM) of the encircled energy function is  $11.5'$  at 0.2 keV, falling to  $5.1'$  at 1 keV. The effective area just below the C edge at 0.28 keV is  $20$  cm<sup>2</sup>. The in-orbit background counting rate is  $9.7 \times 10^{-6}$  arcmin<sup>-2</sup> s<sup>-1</sup> keV<sup>-1</sup>. *BeppoSAX* was launched into a 600 km equatorial orbit on 1996 April 30.

Hale-Bopp was observed by *BeppoSAX* between 1996 September 10 04:55 and September 11 04:21 UTC. The LECS exposure is 11.5 ks. A weak ( $2.1 \pm 0.3$ )  $\times 10^{-12}$  erg cm<sup>-2</sup> s<sup>-1</sup>; 0.1–2.0 keV) source is visible  $3.5'$  off-axis. The source position is  $<2'$  ( $<2.6 \times 10^5$  km) from the comet’s nucleus (see below) and examination of the *ROSAT* All Sky Survey catalog (Voges et al. 1996) reveals no known X-ray sources at this position. Using the *ROSAT* logN-logS relation of Hasinger et al. (1993) the probability of randomly detecting an X-ray source as bright as this within the extraction region is  $6 \times 10^{-3}$ . We exclude a UV leak as being responsible for the counts since the LECS has made a number of deep observations of UV bright stars such as Polaris and Capella and no unexpected features were found. In addition, there are no unusual objects in the SIMBAD database and inspection of several deep LECS exposures revealed no “hot spots”, or other instrumental features at this position. The Medium Energy Concentrator Spectrometer (MECS; 1.3–10 keV; Boella et al. 1997b) detected excess 1.3–2.0 keV emission at a position consistent with the LECS detection (at  $1.3\sigma$  confidence) with an intensity of  $(3.3 \pm 2.5) \times 10^{-14}$  erg cm<sup>-2</sup> s<sup>-1</sup>. This is in good agreement with LECS 1.3–2.0 keV intensity of  $(1.8 \pm 1.1) \times 10^{-14}$  erg cm<sup>-2</sup> s<sup>-1</sup>. Based on the above, we identify comet Hale-Bopp as the source of the detected X-rays.

A motion corrected image of the region of sky containing Hale-Bopp is shown in Fig. 1. The image is re-binned to a  $56'' \times 56''$  pixel size and smoothed using a Gaussian filter of width  $1'.5$  ( $1.9 \times 10^5$  km). The direction of the comet's motion and the position of the Sun are indicated. The bulk of the emission originates on the sunward side of the comet in agreement with *ROSAT* images of comet Hyakutake (Lisse et al. 1996). The extent of the emission is consistent with the LECS point spread function (PSF) of  $9'.5$  FWHM at the mean energy of the detected emission, although the width normal to the Sun-nucleus axis appears wider than in the direction of motion, similar to that observed in other comets. The 68% confidence limit to any source extent is  $<6'.5$  or  $<8.1 \times 10^5$  km. At the start of the LECS observation, the source position is RA =  $17^{\text{h}} 33^{\text{m}} 43^{\text{s}}.4$ , decl. =  $-6^{\circ} 01' 12''$  (J2000) with a 68% confidence uncertainty radius of  $1'.0$ . This is  $1'.7 \pm 1'.0$ , or  $(2.1 \pm 1.3) \times 10^5$  km, from the position of the nucleus, in the general solar direction.

The source spectrum was extracted from within an  $8'$  radius of the mean source position and analyzed using version 1.4.0 of the SAXLEDAS data analysis system. No correction for the comets  $17'' \text{ hr}^{-1}$  motion was applied since most of the events arrive within the first  $3 \times 10^4$  s (see Fig. 2) when the movement of  $<2'.5$  is small compared to the size of the extraction region. The total number of counts is 246, whereas 113 are obtained at the same position in the standard background exposure. The comet's position at the time of the LECS observation was near the southern tip of the North Polar Spur. The low-energy X-ray background in this area is higher than in the areas used in the standard LECS background field (*e.g.*, Snowden et al. 1995). For this reason the background spectrum was extracted from the image itself using an  $8'$  radius region centered  $16'$  diametrically opposite in the LECS FOV. A small correction for mirror vignetting was applied. After background subtraction, the count rate is  $0.0120 \pm 0.0018 \text{ s}^{-1}$ .

The extracted spectrum is equally well fit (with  $\chi^2$ 's of 9 for 9 degrees of freedom (dof)) by a thermal bremsstrahlung model of temperature  $0.29 \pm 0.06$  keV or a power-law model of photon index  $3.1 \pm_{0.2}^{0.6}$  (Fig. 3). A blackbody gives a less acceptable fit with a  $\chi^2$  of 18 for 9 dof ( $P(>\chi^2)=3\%$ ). The 0.1–2.0 keV spectrum predicted by the Solar wind model of Häberli et al. (1997) was also fit to the LECS data. This spectrum consists of a series of narrow lines resulting from the excitation of highly charged states of O, C, and Ne ions (see Table 2 of Häberli et al. 1997). The line species are not expected to vary appreciably from comet to comet, and so the line energies were fixed at the values given in Häberli et al. (1997). The best-fit  $\chi^2$  is 44 for 6 dof, with 3 of the lines requiring zero flux. The 95% confidence limits to C and O narrow line emission at 0.28 and 0.53 keV are  $1.0 \times 10^{15}$  and  $7.8 \times 10^{15} \text{ erg s}^{-1}$ , respectively. This implies that any such narrow line luminosity must be  $<18\%$  of the 0.1–2.0 keV continuum luminosity.

The 0.1–2.0 keV luminosity is  $4.8 \times 10^{16}$  erg s<sup>-1</sup>, or  $2.1 \times 10^{-12}$  erg cm<sup>-2</sup> s<sup>-1</sup>, for the best-fit thermal bremsstrahlung spectrum and  $5.9 \times 10^{16}$  erg s<sup>-1</sup>, or  $2.6 \times 10^{-12}$  erg cm<sup>-2</sup> s<sup>-1</sup>, for the best-fit power-law spectrum. Using the 0.07–0.18 keV *EUVE* Deep Survey camera, Krasnapolsky et al. (1997), assuming spectrally uniform emission, derive 0.095–0.165 keV fluxes of  $8 \times 10^{24}$  and  $1.5 \times 10^{25}$  photons s<sup>-1</sup> for radii of  $4 \times 10^5$  and  $10^6$  km, respectively. This narrower energy range is used by Krasnapolsky et al. (1997) to reflect the “effective” instrument bandpass. In addition, the LECS source is point-like (with an extent of  $<8.1 \times 10^5$  km), while that observed by *EUVE* is extended. It is therefore not straightforward to compare LECS and *EUVE* fluxes. Using the *EUVE* flux within the upper-limit LECS source extent, gives a LECS to *EUVE* flux ratio of  $8.3 \pm 1.4$ . (Note, the *EUVE* flux was derived assuming spectrally uniform emission.) Using the larger source radius reduces this ratio to  $4.4 \pm 1.0$ . The above uncertainties include the contribution from the error on the LECS temperature determination. Although the measured extent of the dust cloud ( $\sim 2\text{--}4 \times 10^5$  km) at the time of the *EUVE* observation is comparable to the smaller radius, we take the worst case LECS to *EUVE* flux ratio to be  $>3.4$ .

Figure 2 shows light curves for the same source and background regions as for the spectrum. The integration interval is 2000 s. A best-fit constant count rate to the background region data yields a  $\chi^2$  of 14 for 15 dof, whereas for the source region the  $\chi^2$  is 44 for 13 dof. Figure 2 indicates that the X-ray intensity of the comet gradually decreased during the observation and is variable by a factor of  $\sim 2$  on a timescale of hours. Modeling the light curve by an exponential decay, reduces the  $\chi^2$  to 18 for 12 dof for a 1/e time of 9.3 hr.

### 3. OPTICAL OBSERVATIONS

Contemporary optical observations were carried out on the 2.2 m telescope at La Silla using the multi-mode EFOSC II instrument in 3 narrow bands to differentiate between dust ( $\lambda=4467$  Å ,  $\Delta\lambda=56$  Å FWHM) and C<sub>2</sub> ( $\lambda=5117$  Å ,  $\Delta\lambda=56$  Å FWHM) and CN ( $\lambda=3849$  Å ,  $\Delta\lambda=87$  Å FWHM) gas emissions. Hale-Bopp was observed at about 01:00 UTC on the nights of 1996 September 10 to September 17 with exposure times of 180 s (dust), 180 s (C<sub>2</sub>) and 300 s (CN). Each image was divided by the previous one so that temporal changes in the coma become apparent. This technique removes the strong smooth intensity profile of the coma so that superimposed time variable structures become visible (Schulz 1991).

The quotient images (Fig. 4, top) and differential brightness profiles (the lower panel of Fig. 4) show that a dust cloud was ejected from the nucleus which expanded outwards

and appeared as a shell when integrated over the line of sight. The original images show that the bulk of the dust was emitted towards the North and North-West. Additionally, four jets are apparent in Fig. 4a confirming the observations of Kidger et al. (1996). They are suppressed in subsequent images because the exposures were taken at intervals of very nearly twice the rotation period ( $\sim 11.5$  hr) of the nucleus. The jets are unlikely to be related to the cloud as multiple jets were continually observed during 1996 August and September (Kidger et al. 1996).

The transverse dust velocities were determined by measuring the position of maximum emission in radial brightness profiles derived from the original images (see the lower panel of Fig. 4). By extrapolating backwards, the onset of the outburst occurred on 1996 September 9 ( $9.4 \pm 1$ ) UTC. The thickness of the shell is a function of the outburst lifetime and the velocity distribution of the dust. The images indicate that the outburst lasted for  $\leq 1$  day, after which dust ejection ceased and the shell expanded outwards at an average velocity of  $0.11 \text{ km s}^{-1}$ , becoming increasingly tenuous. The temporal evolution of the dust radial intensity profiles is shown in the lower panel of Fig. 4. The quiescent intensity is taken to be that measured  $2 \times 10^5 \text{ km}$  from the comet on 1996 September 10. This distance is a factor of  $\sim 10$  times further than the outburst dust had traveled, and so provides an uncontaminated measure. Assuming the dust column density is proportional to its optical intensity, the ratio of maximum to quiescent intensities gives an estimate of the change in dust column density. This is at least a factor of 7 greater at the time of the LECS observation. After September 10, the dust cloud density decreased at an initial rate of  $\simeq 40\%$  per day as the shell expanded outwards. On September 11 the cloud had an angular extent of  $\sim 0.8'$  or  $\sim 10^5 \text{ km}$  and by the start of the *EUVE* observation (September 14), it had increased to  $\sim 2'$  or  $\sim 3 \times 10^5 \text{ km}$ . At this time, the cloud occupied a volume of  $10^{31} \text{ cm}^3$  and the column density of dust had returned to within a factor of 2 of its “quiescent” level. The cloud can hardly be discerned in the CCD image of September 16. *EUVE* continued observing until September 19.

For the gas images, only a CN shell was detected and only on September 10. It had a radial extent about twice that of the dust, but with a relative change in column density of 10 times less. However, CN is a daughter product which is believed to be partially released from the dust (A'Hearn et al. 1995) and is therefore not representative of the gas outflow from the nucleus. At these heliospheric distances, dust activity is driven largely by CO and H<sub>2</sub>O emission (Weaver et al. 1997) to which the CCD images are insensitive. Biver et al. (1997) measured the outflow velocities of CO and OH (the main by-product of H<sub>2</sub>O photo-dissociation) around the time of the LECS observation to be  $0.5\text{--}0.7 \text{ km s}^{-1}$  i.e., at least 5 times that of the dust. Additionally, while the nucleus was out-gassing significant quantities ( $\sim 3 \times 10^{29} \text{ s}^{-1}$ ) of both molecules, there is no evidence of a large gas outburst in

the data of Biver et al. (1997). We caution however, that such an event could be missed since the lifetimes of CO and H<sub>2</sub>O are of the order of days, and the data are infrequently sampled.

#### 4. DISCUSSION

The best-fit LECS bremsstrahlung temperature of  $0.29 \pm 0.06$  keV is similar to that determined by *ROSAT* for comets Hyakutake and Tsuchiya-Kiuchi (0.40 keV, Lisse et al. 1996; Dennerl, Englhauser, & Trümper 1996b). Figure 1 indicates that the bulk of the X-ray emission originates on the sunward side of the nucleus, also in agreement with previous observations. The emission may also show a characteristic elongation normal to the Sun-nucleus line. The similarity in properties between the LECS measurement of comet Hale-Bopp and *ROSAT* observations of Hyakutake and Tsuchiya-Kiuchi further supports the view that the X-rays originate from Hale-Bopp. The 0.1–2.0 keV luminosity of  $4.8 \times 10^{16}$  erg s<sup>-1</sup> is a factor 12 greater than observed from comet Hyakutake at a heliocentric distance of 1.0 AU and a factor 2.5 greater than from comet Tsuchiya-Kiuchi at a heliocentric distance of 1.4 AU. As we demonstrate below, the intense X-ray emission observed from comet Hale-Bopp by *BeppoSAX* is probably related to the large amount of dust present at the time.

The LECS spectrum is inconsistent with that expected from models which predict the bulk of emission to be in the form of lines, such as the solar fluorescent and the solar wind charge exchange models. In the case of comet Hyakutake, the plasma turbulence model of Bingham et al. (1997) predicts an O VII 0.57 keV line with an intensity  $\sim 10$  times greater than the underlying bremsstrahlung continuum (Kellett et al. 1997). For comet Hale-Bopp, the 95% confidence upper limit to any such line emission is  $<16\%$  of the 0.1–2.0 keV continuum intensity or  $<10\%$  of the total luminosity. Models which involve perturbations of the solar wind or interplanetary magnetic field can also be excluded by contemporaneous *Geostationary Observational Environmental Satellite-8 (GOES-8)* and *Solar Wind Experiment (SWE)* data which show that the solar X-ray and particle fluxes and the local magnetic field were stable at very low levels around the time of the LECS observation.

Krasnoplosky (1997) has shown that the attogram dust model can successfully explain the measured fluxes from comet Hyakutake. Scaling the Hyakutake X-ray flux by the quiescent gas and dust production rates and heliospheric distances of Hyakutake and Hale-Bopp, the predicted Hale-Bopp X-ray flux is in good agreement with that measured by *EUVIE*, under the assumption that the X-ray emissivities are similar (Krasnopolsky et

al. 1997b). Since X-ray intensity is expected to scale with the amount of dust, at least a factor of 3.4 (and more probably 8) more dust is required to account for the X-ray intensity observed by *BeppoSAX*, assuming the dust size distribution and solar X-ray flux remain the same. The dust production rate before the outburst is estimated to be  $\sim 4 \times 10^4 \text{ kg s}^{-1}$  and the ratio of dust to gas production  $\sim 3$  (Rauer, Arpigny, & Boehnhardt 1997). The estimated dust production rate during the outburst is at least  $3 \times 10^5 \text{ kg s}^{-1}$ , an increase by a factor of  $>7$  compared to before the outburst, sufficient to account for the observed X-ray flux with the attogram dust model. We cannot directly measure the corresponding change in the amount of gas surrounding the comet. However during previous outbursts the gas production rate increased by a factor of only 1–3 depending on the species (Weaver et al. 1997). Since the shell in Fig. 4 is thickening and expanding with time, its density is expected to vary as  $\sim v^{-3}$ , rather than  $v^{-2}$  expected for a shell of constant thickness. Thus, assuming constant gas and dust velocities and spherical outflow, the gas density will decrease  $\sim 200$  times more rapidly than the dust, purely due to its higher expansion velocity.

By the start of the *EUVE* observation the dust density had decreased to a maximum of twice its quiescent level and the cloud had a size of  $\sim 2'$  or  $\sim 3 \times 10^5 \text{ km}$ . By the end of the *EUVE* observation, the cloud filled most of the aperture providing an explanation for the source of extended emission reported in Mumma et al. (1997). The bulk of the dust outburst occurred towards the North and North-West of the nucleus. It is interesting to note that the majority of the X-rays observed by *EUVE* also originated to the North of the nucleus (see Fig. 1 of Krasnopolsky et al. 1997a). The reason that *EUVE* observed a lower flux than *BeppoSAX* is probably a combination of the continuation of the decay of the X-ray flux shown in Fig. 2 and poorer signal-to-noise caused by the spread of the signal over a much larger area of sky. In the absence of a more convincing explanation, we attribute this decay to dust fragmentation to sizes which are increasingly inefficient in producing X-rays.

Based on the following arguments we conclude that the observed X-rays are most likely produced in dust rather than gas. (1) the increase of dust produced during the outburst can explain the X-ray flux measured by the LECS, (2) sub-micron grain sizes have been observed in the coma of Hale-Bopp (Williams et al. 1997), (3) the measured spectrum is inconsistent with that predicted by gaseous models but consistent with that predicted by the attogram dust model, (4) the spatial distribution of X-rays measured by *EUVE* is similar to that of the dust from the outburst, and (5) X-rays were not observed from comet Bradfield 1979X - a highly gaseous but the least dusty comet observed (Hudson et al. 1981).

*GOES-8* data were kindly provided by D. Wilkinson of the NOAA/National Geophysical Data Center and *SWE* data by K.W. Ogilvie (NASA/GSFC), J.T. Steinberg (MIT), and A.J. Lazarus (MIT). K. Dennerl is thanked for many useful conversations. A. Orr and T.

Oosterbroek acknowledge ESA Research Fellowships. The *BeppoSAX* satellite is a joint Italian and Dutch programme.

COMETARY X-RAY EMISSION MODELS

Emission Mechanism	$\epsilon^a$	Ref.
Ionization by solar wind protons	$10^{-6}$	1
Current sheets in the solar wind	$>10^{-6}$	2
High velocity dust-dust collisions	$10^{-5}$	1
X-ray scattering in coma	$10^{-3}$	1
Solar X-ray fluorescence	$10^{-3}$	1
Bremsstrahlung from cometary electrons accelerated by plasma turbulence	$10^{-2}$	3
Charge exchange of heavy solar wind ions with neutral cometary molecules	1	4
Solar X-ray scattering, fluorescence and bremsstrahlung in attogram dust particles	2	1

<sup>a</sup>The ratio of predicted to measured fluxes for comet Hyakutake.

<sup>1</sup>Krasnopolsky 1997; <sup>2</sup>Brandt, Lisse, & Yi 1997; <sup>3</sup>Bingham et al. 1997; <sup>4</sup>Häberli et al. 1997.

## REFERENCES

- A'Hearn, M. F., Millis, R. L., Schleicher, D. G., Osip, D. J., Berch, P. V. 1995, *Icarus*, 118, 223
- Bingham, R., Dawson, J. M., Shapiro V. D., Mendis, D. A., Kellett, B. J. 1997, *Science*, 275, 49
- Biver, N., et al. 1997, *Science*, 275, 1915
- Boella, G., Butler, R. C., Perola, G. C., Piro, L., Scarsi, L., Bleeker, J. A. M. 1997a, *A&AS*, 122, 299
- Boella, G., et al. 1997b, *A&AS*, 122, 327
- Bowyer, S., & Malina, R. F. 1989, in *Extreme Ultraviolet Astronomy*, ed. R. F. Malina & S. Bowyer, Pergamon press, New York, 397
- Brandt, J. C., Lisse, C., & Yi, Y. 1997, *BAAS*, 189, 25.05
- Cravens, T. E. 1997, *Geophys. Res. Lett.*, 24, 105
- Dennerl, K., Englhauser, J., & Trümper, J. 1996a, *IAU Circ.*, 6495
- Dennerl, K., Englhauser, J., & Trümper, J. 1996b, *IAU Circ.*, 6404
- Häberli, R. M., Gombosi, T. I., de Zeeuw, D. L., Combi, M. R., Powell, K. G. 1997, *Science*, 276, 939
- Hale, A., & Bopp, T. 1996, *IAU Circ.*, 6187
- Hasinger, G., Burg, R., Giacconi, R., Hartner, G., Schmidt, M., Trümper, J., Zamorani, G. 1993, *A&A*, 275, 1
- Hudson, H. S., Ip, W. H., Mendis, D. A. 1981, *Planet. Space Sci.*, 29, 1373
- Ibadov, S. 1990, *Icarus*, 86, 283
- Kellett, B., Negoro, H., Nagase, F., Bingham, R., Dawson, J. M., Mendis, D. A., Shapiro, V. D. 1997, preprint
- Kidger, M. R., Serra-Ricart, M., Denicolo, G., Torres-Chico, R., Bellot-Rubio, L. R., Casas, R., Gómez, A., Licandro, J. 1996, *ApJ* submitted
- Krasnopolsky, V. 1997, *Icarus*, submitted

- Krasnopolsky, V. A., et al. 1997a, *Science*, 277, 1488
- Krasnopolsky, V. A., et al. 1997b, *Annales Geophysicae*, 15, supp. III, C802
- Lisse, C. M., et al. 1996, *Science*, 274, 205
- Mumma, M., Krasnopolsky, V. A., Abbott, M., Flynn, B. C., Yeomans, D. K., Feldman, P. D., Cosmovici, C. B. 1997, *IAU Circ.*, 6625
- Owens, A., Oosterbroek, T., Orr, A., Parmar, A. N., Antonelli, L. A., Fiore, F., Maccarone, M. C., Piro, L. 1997, *IAU Circ.*, 6614
- Parmar, A. N., et al. 1997, *A&AS*, 122, 309
- Rauer, H., Arpigny, C., & Boehnhardt, H. 1997, *Science*, 275, 1909
- Schulz, R. 1991, in *Proc. 3rd ESO/ST-ECF Data Analysis Workshop*, ed. P. J. Grossbol & R. H. Warmels (Garching: ESO), 73
- Snowden, S. L., et al. 1995, *ApJ*, 454, 643
- Utterback, N. G., & Kissel, J. 1990, *AJ*, 100, 1315
- Voges, W., et al. 1996, *A&A*, submitted
- Weaver, H. A., et al. 1997, *Science*, 275, 1900
- Wickramasinghe, N. C., & Hoyle, F. 1996, *Ap. Space Sci.*, 239, 121
- Williams, D. M., et al. 1997, *ApJ*, 489, L91

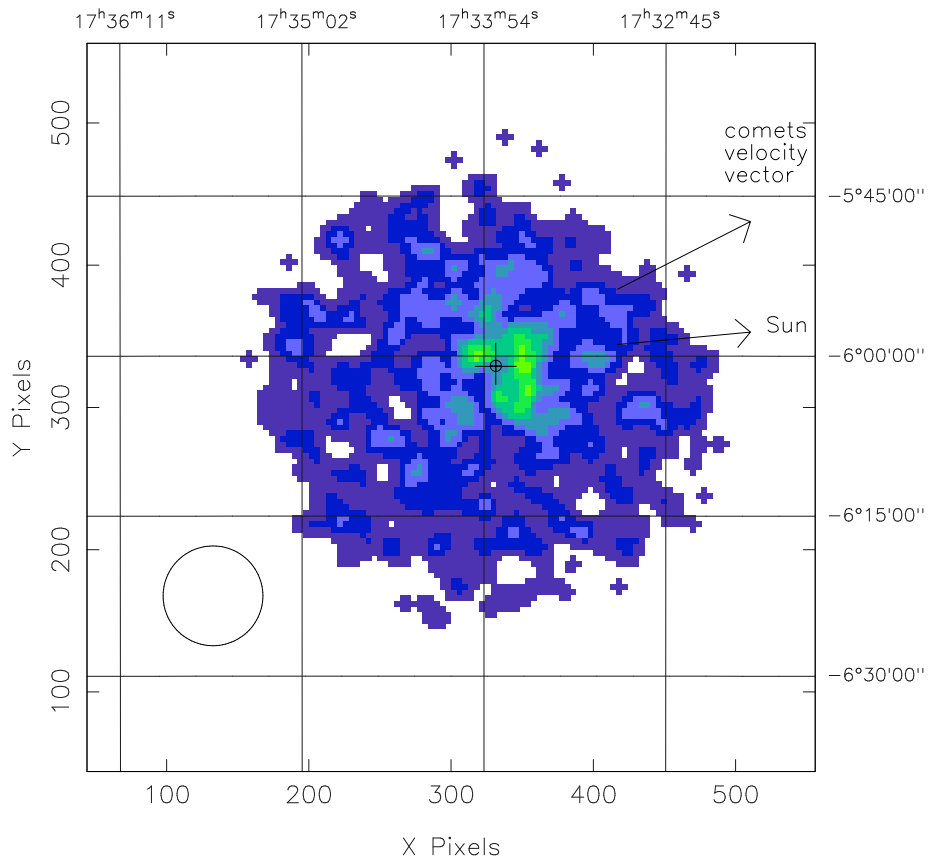


Fig. 1.— A 0.1–2.0 keV image of the sky containing comet Hale-Bopp. The image has been corrected for the motion of the comet ( $\sim 17'' \text{ hr}^{-1}$ ). For comparison, the FWHM of the PSF at the mean energy of the source is indicated by the circle in the lower left hand corner. The position of the nucleus is indicated by the small circle and cross. The position of the Sun and the comet’s velocity vector are indicated.

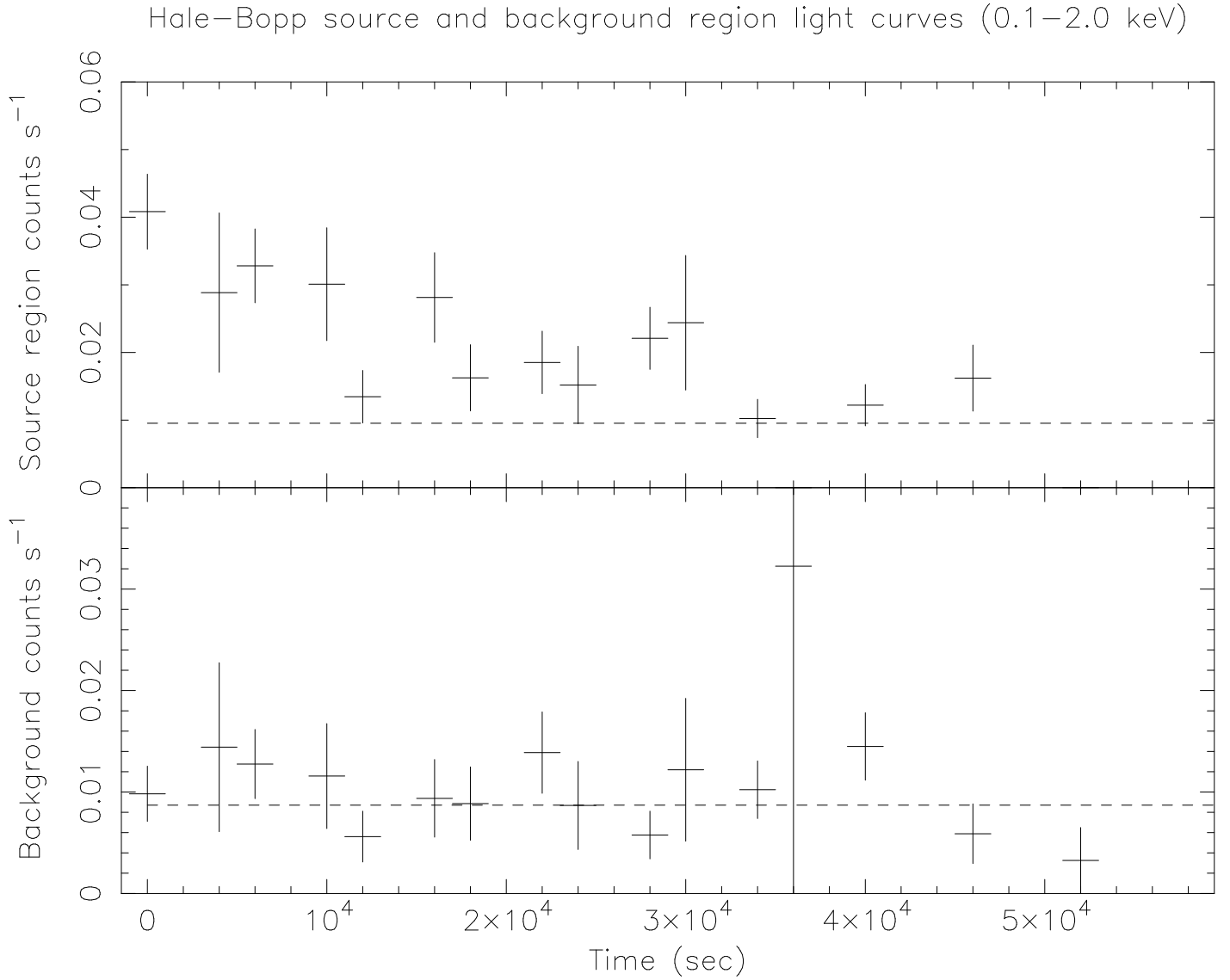


Fig. 2.— The 0.1–2.0 keV light curves of source and background regions. The mean count rate in the background region is shown by the dotted line in the lower panel. Based on this, the predicted background level at the position of the comet (corrected for the difference in vignetting) is indicated by the dotted line in the upper panel.

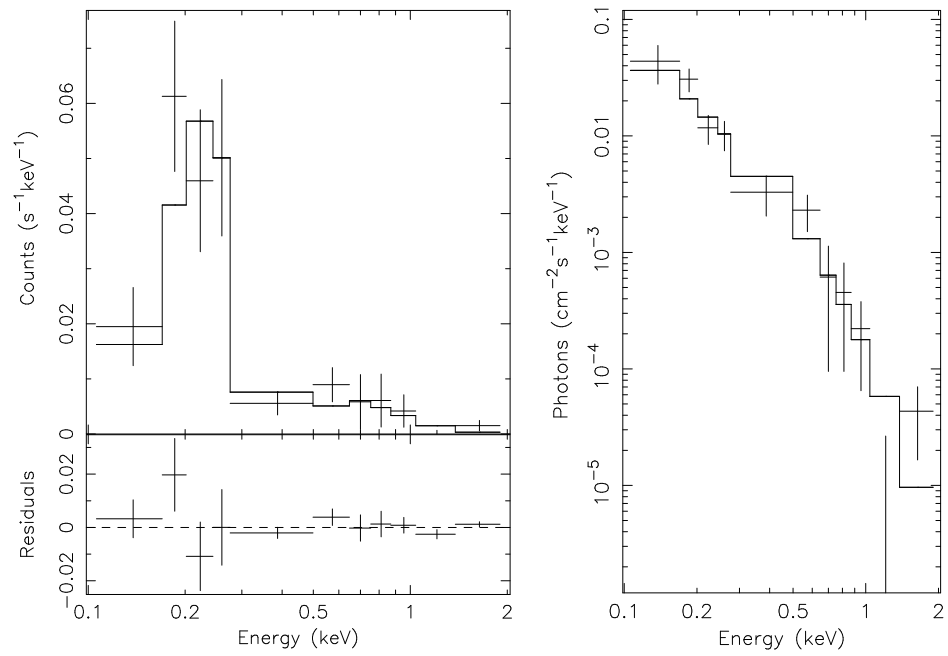


Fig. 3.— The observed LECS Hale-Bopp spectrum and best-fit thermal bremsstrahlung model ( $kT = 0.29$  keV). The lower left panel shows the residuals. The inferred photon spectrum and model prediction are shown in the right panel.

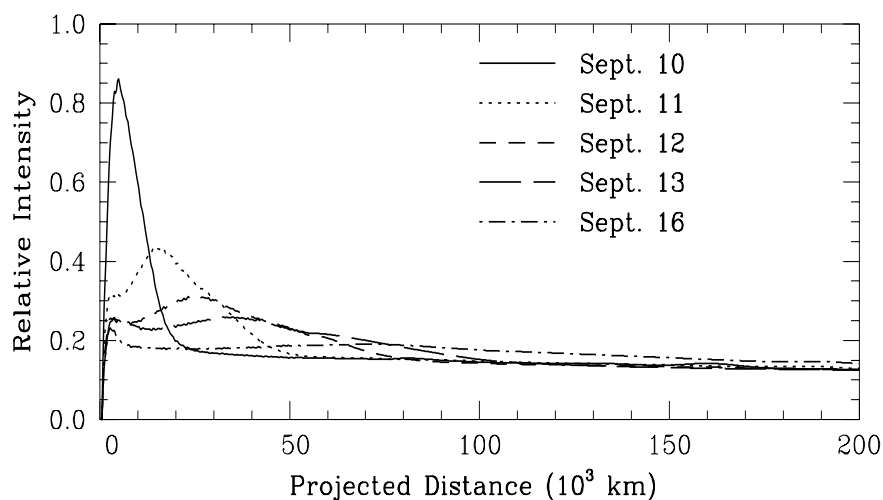
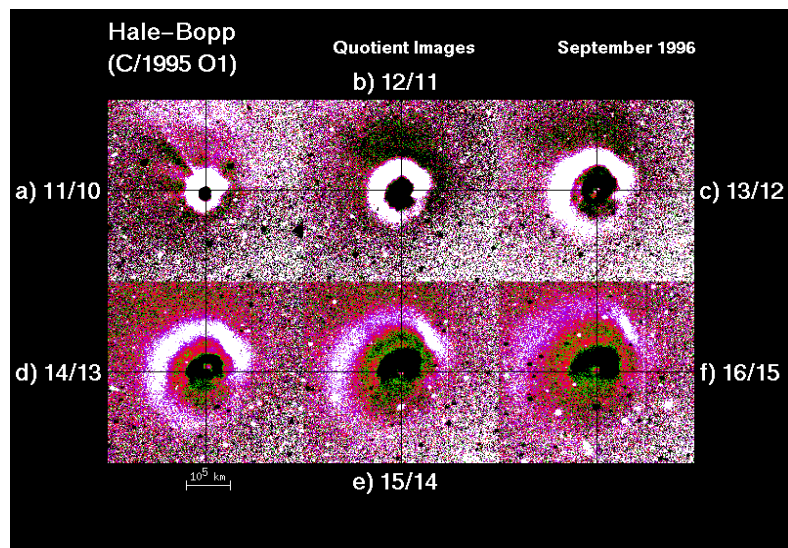


Fig. 4.— The temporal evolution of the dust shell observed in Hale-Bopp between 1996 September 10 and 17. Each image is the ratio between an image and that obtained the previous day and thus highlights changes between consecutive days. The images have the same orientation as Fig. 1. The intensity coding of the quotient images has been modified to enhance the resulting shell in each case. White indicates a large change and black no change. Note, as the shell is expanding with time, each image is divided by one with a smaller and more intense shell. This artificially increases the dimension of expanding shell structures and hence the apparent expansion velocity of the shell. Lower panel: Differential dust band ( $\lambda=4467 \text{ \AA}$ ) radial intensity profiles obtained by differentiating the intensities in concentric circular apertures centered on the maximum intensities in the dust coma. A clear evolution of the dust shell is evident. The ratio of the peak intensity on September 10 and the quiescent value (as measured  $2 \times 10^5 \text{ km}$  from the comet on 1996 September 10) implies a change in the dust column density by at least a factor a 7.